62. Shafi, Q. & Vilenkin, A. *Phys. Rev. Lett.* **52,** 691–694 (1984).
63. Steinhardt, P. J. & Turner, M. S. Preprint (Fermilab, 1984).
64. Quinn, H. R. & Gupta, S. *Phys. Rev.* **D29,** 2791–2797 (1984).
65. Zeldovich, Ya. B. *Mon. Not. R. astr. Soc.* **192,** 663–667 (1980).
66. Vilenkin, A. *Phys, Rev.* **D24,** 2082–2089 (1981).
67. Bond, J. R., Efstathiou, G. & Silk, J. *Phys. Rev. Lett.* **45,** 1980–1984 (1980).
68. Doroshkevich, A. G., Zeldovich, Ya. B., Sunyaev, R. A. & Khlopov, M. Yu. *Soviet Astr. Lett.* **6,** 252–256 (1980).
69. Chernin, A. D. *Soviet Astr.* **25,** 14–16 (1981).
70. White, S. D. M. & Rees, M. J. *Mon. Not. R. astr. Soc.* **183,** 341–358 (1978).
71. Rees, M. J. & Ostriker, J. P. *Mon. Not. R. astr. Soc.* **179,** 541–559 (1977).
72. Faber, S. M. *Astrophysical Cosmology: Proc. Study Week on Cosmology and Fundamental Physics* (eds Brück, H. A., Coyne, G. V. & Longair, M. S.) 191–234 (Pontifical Scientific Academy, Vatican, 1982).
73. Silk, J. *Nature* **301,** 574–578 (1983).
74. Forman, W. & Jones, C. *Ann. Rev. Astr. Astrophys.* **20,** 547–585 (1982).
75. Geller, M. J. & Beers, T. C. *Proc. Astr. Soc. Paci.* **94,** 421–439 (1982).
76. Thuan, T. X. & Romanishin, W. *Astrophys. J.* **248,** 439–459 (1981).
77. Cavaliere, A., Santangelo, P., Tarquini, G. & Vittorio, N. *Clusters and Groups of Galaxies* (eds Mardirossian, F., Giuricin, G. & Mezzetti, M.) (Reidel, Dordrecht, in the press).
78. Yoneyama, T. *Publ. Astr. Soc. Jap.* **24,** 87–98 (1972).
79. Peebles, P. J. E. Preprint (Princeton Univ., 1984).
80. Fall, S. M. & Rees, M. J. (in preparation).
81. Fall, S. M. & Rees, M. J. *Mon. Not. R. astr. Soc.* **181,** 37P–42P (1977).
82. Geller, M. & Huchra, J. *Astrophys. J. Suppl.* **52,** 61–87 (1983).
83. Faber, S. M., Blumenthal, G. R. & Primack, J. R. *Astrophys. J. Lett.* (submitted).
84. Blumenthal, G. R., Faber, S. M. & Primack, J. R. (in preparation).
85. Efstathiou, G. & Jones, B. J. T. *Mon. Not. R. astr. Soc.* **186,** 133–144 (1979).
86. Fall, S. M. & Efstathiou, G. *Mon. Not. R. astr. Soc.* **193,** 189–206 (1980).
87. Sandage, A., Freeman, K. C. & Stokes, N. R. *Astrophys. J.* **160,** 831–844 (1970).
88. Efstathiou, G. & Barnes, J. *Formation and Evolution of Galaxies and Large Scale Structures in the Universe* (eds Audouze, J. & Tran Thanh Van, J.) 361–377 (Reidel, Dordrecht, 1984).
89. Gott, J. R. & Thuan, T. X. *Astrophys. J.* **204,** 649–667 (1976).
90. Davis, M. & Peebles, P. J. E. *Astrophys. J.* **267,** 465–482 (1983).
91. Sandage, A. *Proc. 1st ESO–CERN Symp., Large Scale Structure of the Universe, Cosmology, and Fundamental Physics* (in the press).
92. Davis, M., Efstathiou, G., Frenk, C. & White, S. D. M. (in preparation).
93. Bond, J. R. & Efstathiou, G. Preprint (NSF-ITP-84-79, 1984).
94. Vittorio, N. & Silk, J. Preprint (U. Cal. Berkeley, 1984).
95. Peebles, P. J. E. Preprint (Princeton Univ., 1984).
96. Kaiser, N. *Inner Space/Outer Space* (eds Kolb, E. W. *et al.*) (University of Chicago Press, in the press).
97. Bardeen, J. *Inner Space/Outer Space* (eds Kolb, E. W. *et al.*) (University of Chicago Press, in the press).
98. Hoffman, G. L., Salpeter, E. E. & Wasserman, I. *Astrophys. J.* **268,** 527–539 (1983).
99. Hoffman, Y. & Shaham, J. *Astrophys. J. Lett.* **262,** L23–L26 (1982).
100. Kirshner, R. F., Oemler, A., Schechter, P. L. & Schectman, S. A. *Astrophys. J. Lett.* **248,** L57–L60 (1981).
101. Kirshner, R. F., Oemler, A., Schechter, P. L. & Schectman, S. A. *Early Evolution of the Universe and its Present Structure, IAU Symp.* No. 104 197–202 (1983).
102. Oort, J. H. *A. Rev. Astr. Astrophys.* **21,** 373–428 (1983).
103. Dressler, A. *Astrophys. J.* **236,** 351–365 (1980).
104. Postman, M. & Geller, M. J. *Astrophys. J.* **281,** 95–99 (1984).
105. Binggeli, B. *Astr. Astrophys.* **107,** 338–349 (1982).
106. Zeldovich, Ya. B. *Astr. Astrophys.* **5,** 84–89 (1970).
107. Arnold, V. I., Shandarin, S. F. & Zeldovich, Ya. B. *Geophys. Astrophys. Fluid Dyn.* **20,** 111 (1982).
108. Bond, J. R., Centrella, J., Szalay, A. S. & Wilson, J. R. *Formation and Evolution of Galaxies and Large Structures in the Universe* (eds Audouze, J. & Tran Thanh Van, J.) 87–99 (Reidel, Dordrecht, 1984).
109. Shapiro, P. R., Struck-Marcell, C. & Melott, A. L. *Astrophys. J.* **275,** 413–429 (1983).
110. Dekel, A., West, M. J. & Aarseth, S. J. *Astrophys. J.* **279,** 1 (1984).
111. Melott, A., Einasto, J., Saar, E., Suisalu, I., Klypin, A. A. & Shandarin, S. F. *Phys. Rev. Lett.* **51,** 935–938 (1983).
112. Dekel, A. *Astrophys. J.* **264,** 373–391 (1983).
113. Doroshkevich, A. G., Shandarin, S. F. & Zeldovich, Ya. B. *Commt Astrophys.* **9,** 265–273 (1982).
114. Rees, M. J. *Clusters and Groups of Galaxies* (eds Mardirossian, F., Giuricin, G. & Mezzetti, M.) (Reidel, Dordrecht, in the press).
115. Ostriker, J. P. *Astrophysical Cosmology: Proc. Study Week on Cosmology and Fundamental Physics* (eds Brück, H. A., Coyne, G. V. & Longair, M. S.) 473–493 (Pontifical Scientific Academy, Vatican, 1982).
116. Dekel, A. *8th Johns Hopkins Workshop on Current Problems in Particle Theory* (eds Domokos, G. & Kovesi-Domokos, S.) (World Scientific Publishing, Singapore, in the press).
117. Shandarin, S. F. *Soviet Astr. Lett.* **9,** 104 (1983).
118. Barrow, J. D. & Bhavsar, S. P. *Mon. Not. R. astr. Soc.* **205,** 66 (1983).
119. Dekel, A. & West, M. J. Preprint (NSF-ITP-84-44, 1984).
120. Dressler, A. *Astrophys. J.* **226,** 55–69 (1978).
121. Jones, C. & Forman, W. *Astrophys. J.* **276,** 38–55 (1983).
122. Kriss, G. A., Cioffi, D. F. & Canizares, C. R. *Astrophys. J.* **272,** 439–448 (1983).
123. Beers, T. C., Geller, M. J., Huchra, J. P., Latham, D. W. & Davis, R. J. *Astrophys. J.* (in the press).
124. Gunn, J. E. *Astrophysical Cosmology* (eds Brück, H. A., Coyne, G. V. & Longair, M. S.) 233–259 (Pontifical Scientific Academy, Vatican, 1982).
125. Young, P. J. *Astr. J.* **81,** 807–816 (1976).
126. Kent, S. M. & Gunn, J. E. *Astr. J.* **87,** 945–971 (1982).
127. Kent, S. M. & Sargent, W. L. W. *Astr. J.* **88,** 697–708 (1983).
128. de Vaucouleurs, G., de Vaucouleurs, A. & Corwin, H. R. *2nd Reference Catalogue of Bright Galaxies* (University of Texas, Austin, 1976).
129. Dressler, A. & Sandage, A. R. *Astrophys. J.* **265,** 664–680 (1983).
130. Rubin, V. C. *Internal Kinematics and Dynamics of Galaxies* (ed. Athanassoula, E.) 3–6 (Reidel, Dordrecht, 1983).
131. Rubin, V. C., Ford, W. K., Thonnard, N. & Burstein, D. *Astrophys. J.* **261,** 439–456 (1982).
132. Burstein, D., Rubin, V. C., Thonnard, N. & Ford, W. K. *Astrophys. J.* **253,** 70–85 (1982).
133. Thuan, T. X. & Seitzer, P. O. *Astrophys. J.* **231,** 680–687 (1979).
134. Tonry, J. & Davis, M. *Astrophys. J.* **246,** 680–695 (1981).
135. Raymond, J. C., Cox, D. P. & Smith, B. W. *Astrophys. J.* **204,** 290–292 (1976).
136. Dalgarno, A. & McCray, R. A. *A. Rev. Astr. Astrophys.* **10,** 375–426 (1972).

ARTICLES

Ultrahigh gradient particle acceleration by intense laser-driven plasma density waves

C. Joshi*, W. B. Mori*, T. Katsouleas*, J. M. Dawson*, J. M. Kindel† & D. W. Forslund†

* University of California Los Angeles, California 90024, USA
† Los Alamos National Laboratory, Los Alamos, New Mexico 87545, USA

Space-charge waves driven by resonantly beating two laser beams in a high-density plasma can produce ultrahigh electric fields that propagate with velocities close to c. By phase-locking particles in such a wave, particles may be accelerated to very high energies within a very short distance.

DURING the past four decades, we have witnessed an increase of six orders of magnitude in the output energy of high-energy accelerators, while the cost per MeV has been reduced by a factor of 16 per decade. But can this progress continue? Current accelerators, such as the Stanford linac, have accelerating fields of 200 keV cm^{-1}. However, for particle energies beyond 10 TeV, one had to invent schemes that can produce fields of at least 10 MeV cm^{-1}. In any particle accelerator scheme, the basic requirement for obtaining particles with ultrahigh energies is an intense longitudinal electric field that interacts with particles for a long time. Since highly relativistic particles move nearly at the speed of light c, the energy gained by the particles, $\int E \cdot dl$, is maximum if the field is made to propagate with the particles. Extremely large electric fields propagating with phase velocities close to c can be produced by space charge waves in a plasma (ionized gas). The maximum electric field that can be produced by such a wave is approximately $\sqrt{n_e}$ V cm^{-1}, where n_e is the plasma electron density per cm^3. Thus for plasma densities in the range 10^{16}–10^{20} electrons cm^{-3}, the longitudinal electric fields E_L, can be as large as 10^8–10^{10} V cm^{-1}. We now show that such high-gradient, high-phase velocity plasma density waves can be driven by intense laser beams. If particles could be phase-locked in such waves, this scheme has the potential for accelerating particles to ultrahigh energies in very short distances.

Theory

If an intense laser beam is propagated in a plasma, then in certain conditions, the transverse electric field of the laser (which may reach values of 10^9–10^{10} V cm^{-1}) can be very effectively transformed into a longitudinal electric field of a plasma density wave. In the laser accelerator scheme known as the 'Plasma beat

wave accelerator' proposed by Tajima and Dawson[1,7], such a plasma wave can be driven by beating two colinear laser beams, with frequencies and wavenumbers (ω_0, k_0) and (ω_1, k_1), in a plasma resonantly, such that the frequency and the wavenumber of the plasma wave are

$$\omega_{epw} = \omega_0 - \omega_1$$
$$k_{epw} = k_0 - k_1 \quad (1)$$

To achieve the ultrahigh accelerating gradients, high-density plasmas ($10^{16} < n_e < 10^{20}$ cm^{-3}) must be used. Also, because the laser of frequency ω_0 cannot penetrate a plasma whose density exceeds the critical density n_c, corresponding to the plasma frequency $\omega_p = \omega_0$, plasmas with densities less than the quarter critical density must be used. Physically, the plasma wave consists of regions of space charge, which propagate with a phase velocity v_{ph} that is equal to the group velocity of the beat wave $v_g = c(1 - \omega_p^2/\omega_0^2)^{(1/2)}$. These arise because the spatial intensity gradient of the beat wave envelope, which is in the direction of propagation, exerts a periodic force (ponderomotive force) on the plasma at wavenumber k_{epw}. The plasma wave is thus an electrostatic wave with $\mathbf{E}_{epw}$ parallel to $\mathbf{k}_{epw}$.

When two parallel propagating laser beams beat in a plasma resonantly, the plasma density fluctuations grow rapidly. Using fluid equations it can be shown that for $v_0/c \ll 1$, the plasma wave electric field, which is proportional to the perturbed density, initially grows in time with a growth rate

$$\delta = \left(\frac{1}{4}\frac{v_0(0)}{c}\frac{v_0(1)}{c}\omega_p\right) \text{s}^{-1} \quad (2)$$

where $[v_0(0, 1)]/c = eE_{(0,1)}/m\omega_{(0,1)}c$ is the normalized oscillatory velocity of an electron in the laser field. Wavebreaking is approached when the perturbed density becomes as large as the initial density; however, to reach this limit the plasma wave must remain in phase with the beat wave. As the plasma wave grows, the relativistic effect on the frequency mismatch becomes important[2] and the plasma wave saturates at a lower amplitude given by

$$\varepsilon = \frac{eE_{epw}}{m\omega_{epw}c} = \left(\frac{16}{3}\frac{v_0(0)}{c}\frac{v_0(1)}{c}\right)^{1/3} \quad (3)$$

Once the saturation amplitude is reached, the plasma wave amplitude actually begins to decrease, if this process alone acts to sustain the plasma wave[3].

As the plasma wave is an electrostatic wave, we can use Poisson's equation, $E_{epw} = 4\pi en_e/k_{epw}$, to estimate the maximum electric field that we might expect if we assume that the perturbed electron density is equal to the initial density (the so-called cold plasma wavebreaking limit $\varepsilon = 1$). As the plasma wave is propagating at relativistic speed, the Lorentz transformation gives the maximum energy gained by an electron with initial energy $\gamma_{ph}mc^2$ as $2\gamma_{ph}^2mc^2$ or (n_c/n_e) MeV in a distance $2\gamma_{ph}^2c/\omega_p$. Here, $\gamma_{ph} = (\omega_0/\omega_p)$. For a given laser wavelength, the maximum energy gained increases as the plasma density is reduced but because the electric field scales as $\sqrt{n_e}$ it takes longer and longer to obtain this energy.

In a practical accelerator, we cannot use wavebreaking electric fields because as the electric field approaches this value it 'traps' background plasma electrons and begins to accelerate them. It also develops harmonics. Both of these effects are not desirable if we wish to accelerate an externally-injected bunch of electrons. Computer simulations (described below) show that a coherent plasma wave, without any significant number of self-trapped particles, can be generated with electric fields of the order of 10% of the wavebreaking electric field. If we require that the minimum value of the longitudinal field be 10 MeV cm^{-1}, this leads to a minimum plasma density of 10^{16} cm^{-3}. Using a CO_2 laser to excite a beat wave in such a plasma, gives maximum particle energies of ~100 MeV. The physical reason for this limit on the maximum energy is the dephasing of particles and the electric field of the correct polarity (which only exists for half-a-wavelength of the plasma wave in the wave frame). Although for a given plasma density the maximum energy scales inversely with square of the laser wavelength λ, it becomes increasingly difficult to keep the laser beam focused at shorter wavelengths because the Rayleigh length scales as λ. In a single stage, therefore, the best that can probably be achieved is to accelerate electrons to a few GeV using a laser with wavelength in the micrometre range.

To obtain higher energies, one has to be prepared for multi-staging or invent a scheme for phase-locking the particles in the wave so that they do not out run the wave. One such scheme will be described later.

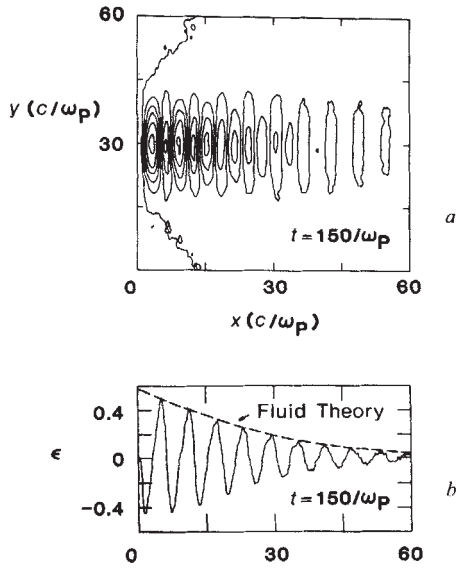

Fig. 1 Potential contours of the space-charge density wave driven by the two laser beams at time $150/\omega_p$ (*a*) section through the centre of the longitudinal electric field of the plasma wave (*b*). The dotted line in *b* shows a comparison of the rate of plasma wave build-up as predicted by the fluid theory with that obtained in these two-dimensional simulations.

Simulations

Computer simulations were carried out using the two-dimensional fully relativistic, electromagnetic particle code WAVE[4] to study the above described acceleration mechanism in a self-consistent manner. A typical WAVE simulation has 10^6 electrons and 10^6 ions. From the particle positions and velocities, charge densities and current densities are found. Then Maxwell's equations are used to calculate the electric and magnetic fields or equivalently the forces on the particles. Equations of motion are used, to calculate new particle locations and velocities and then the process is repeated.

The results of a typical two-dimensional simulation are depicted in Figs 1-3. The parameters for this simulation were as follows: two laser beams $\omega_0 = 5\omega_p$ and $\omega_1 = 4\omega_p$, each with an r.m.s. intensity of $v_0 = 0.4$ *c*, a transverse intensity profile of $\cos^2 y$ and a beam width of 30 c/ω_p were injected into a homogeneous plasma 60 c/ω_p long and 60 c/ω_p wide with a temperature of 2.5 keV. The laser beams had a cubic rise from zero to maximum intensity in $300/\omega_p$ after which the laser intensity remained constant. The ion-to-electron mass ratio was 1,836 and temperature ratio was 1. Thus for an IR laser with wavelengths 9.6 μm and 12 μm the parameters were: a hydrogen plasma with $n_e \sim 4.9 \times 10^{17}$ cm^{-3}, laser risetime ~7.6 ps, laser intensity $\sim 2 \times 10^{15}$ W cm^{-2}, beam width ~25 wavelengths and system length ~50 wavelengths. The simulation parameters were chosen to study both the beat wave driven plasma wave and other competing one- and two-dimensional effects.

The simulation results can be categorized into two time regimes. The first, during the risetime of the laser pulse when

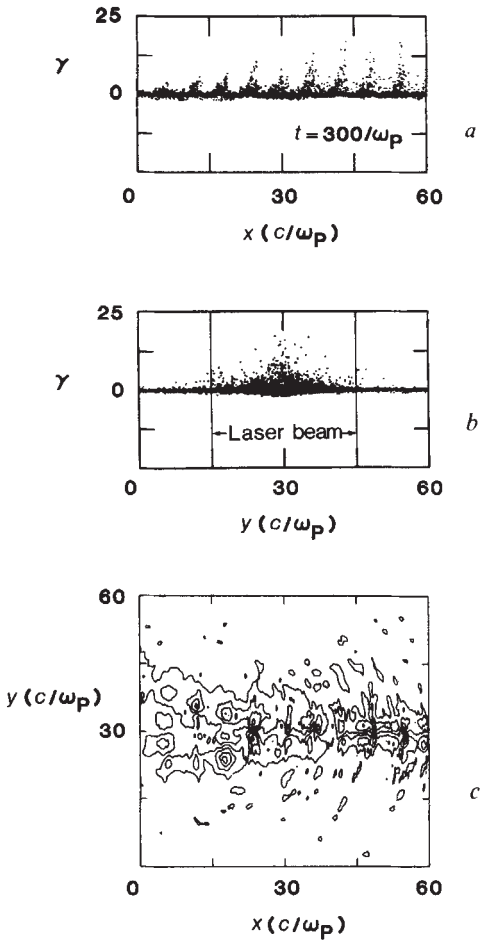

Fig. 2 Phase space plot (momentum in the x direction) of the plasma electrons shows that at time $300/\omega_p$, trapped electrons are accelerated in every wavelength of the plasma wave which represents an accelerating 'bucket' (a). Particles have larger energies on the right-hand side as they have seen an accelerating field for a longer time. The maximum particle energies of $\gamma = 25$ are in good agreement with theory. In the transverse direction, although the laser beam is 30 c/ω_p wide, most particles are confined to a narrow region down the centre of the accelerating wave (b). Contours of the self-consistent magnetic field at time $t = 300/\omega_p$ generated by the accelerating trapped particles (c). This field exerts a radial force on the trapped particles confining them in a small region down the axis and also forces the return current to flow on the outside of the region where it exists.

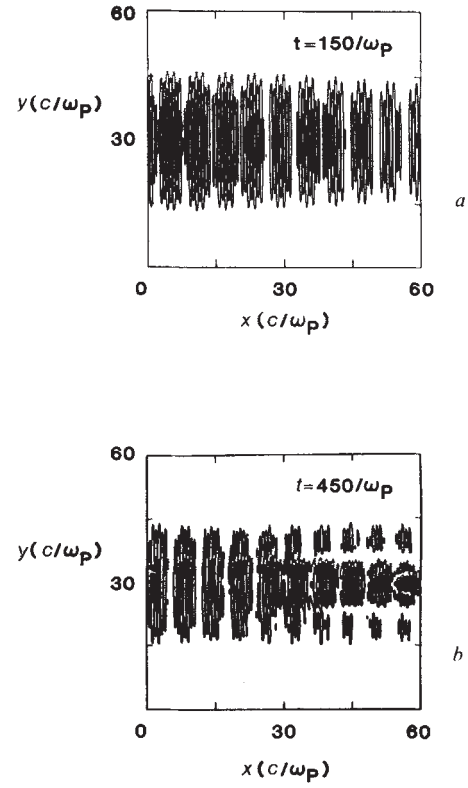

Fig. 3 Contour plot of the beat pattern produced by two colinearly-propagating laser beams in the plasma at time $150/\omega_p$ (a) and at $450/\omega_p$ (b). The x and y dimensions are in units of c/ω_p. Clear evidence for laser beam self-focusing is seen at the later time from the converging inner contours. As a result of self-focusing, the plasma is pushed out and the space-charge wave accelerating the particles disrupts.

a very coherent plasma wave grows and reaches saturation and the second after the peak of the laser pulse ($300/\omega_p$) when competing phenomena come into play.

Figure 1a shows the contour plot of the potential of the plasma density wave at $150/\omega_p$. According to the fluid theory, the plasma wave should reach peak amplitude at this time. The plasma wave wavefronts in the contour plot are seen to be planar. A section through the centre of the transverse axis of the longitudinal electric field plot is shown in Fig. 1b. An extremely coherent plasma wave builds up rapidly in time/space and saturates at $\varepsilon \simeq 0.5$, in excellent agreement with the value expected from the fluid theory. By $300/\omega_p$, the longitudinal electric field becomes non-planar as the laser beams begin to self-focus. Fluid theory would predict that one saturation is reached, the plasma wave amplitude decreases but simulations show that a 'plasma wave' with greatly reduced coherence persists driven by the multiple Raman forward scattering.

Figure 2a shows that the electrons trapped at an earlier time, when the plasma wave field was intense and coherent, have by time $300/\omega_p$ approached maximum energies. Accelerated particles leaving the right-hand boundary of the plasma (not shown here) have maximum energies of $\gamma = 25$, in reasonable agreement with theory. Here $\gamma = (1-\beta^2)^{-1/2}$ is the usual relativistic scaling factor. More important, however, is the fact that although the laser beam and, therefore, the plasma wave is 30 c/ω_p wide, most of the accelerated particles are collimated within 10 c/ω_p of the centre (Fig. 2b). The accelerating particles remain highly collimated because the trapped particles give rise to an azimuthal magnetic field which, in turn, exerts a radial force on the particles keeping them tightly focused. The contour plot of this self-generated magnetic field which can reach megagauss magnitudes is shown in Fig. 2c. The maximum field is in the regions where bunches of electrons are accelerated. The accelerated particles constitute a flow of charges or current which leaves the plasma positively charged, thus driving a return current of colder particles in the opposite direction. In the simulations the return current is found to flow predominantly on the outside of the region bounded by the self-generated magnetic field.

These two-dimensional simulations also allowed us to investigate competition between the beat wave driven plasma wave and Raman back- and side-scattering. To allow the growth of large angle side-scattering the transverse dimension of the beam was made periodic. Even in relatively cold plasmas ($T_e \sim$ 200 eV), where Landau damping is expected to be weak, Raman backscatter is not found to be a problem under two-frequency illumination. Small angle (from the forward direction) side-scatter can occur, effectively making the desired plasma wave non-planar. This gives rise to a radial component of the electric field; however, the self-generated magnetic field tends to keep the trapped particles focused in the centre of the plasma wave as discussed above.

Figure 3a shows the laser beat wave contours at $150/\omega_p$ as the beams propagate from left to right. Contrast this with laser

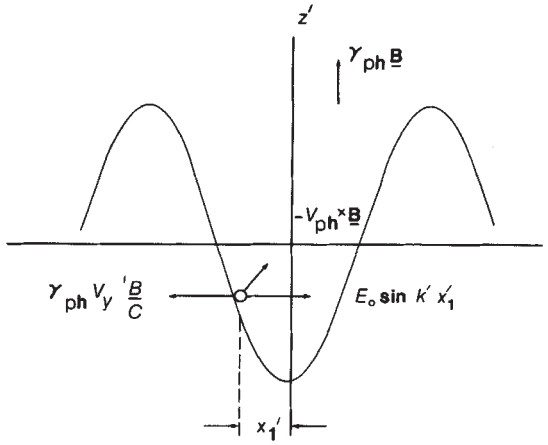

Fig. 4 In the phase stabilization scheme, Surfatron, a perpendicular magnetic field is applied to the wavevector of the longitudinal space-charge wave. In the wave frame, a trapped particle comes to an equilibrium position against the side of the potential well where the 'trapping' and 'de-trapping' forces balance: $E_0 \sin k'_{epw} x' \simeq \gamma_{ph} B$. The energy gained by the particle in the direction of the wave is simply $\gamma_{ph} Bx$.

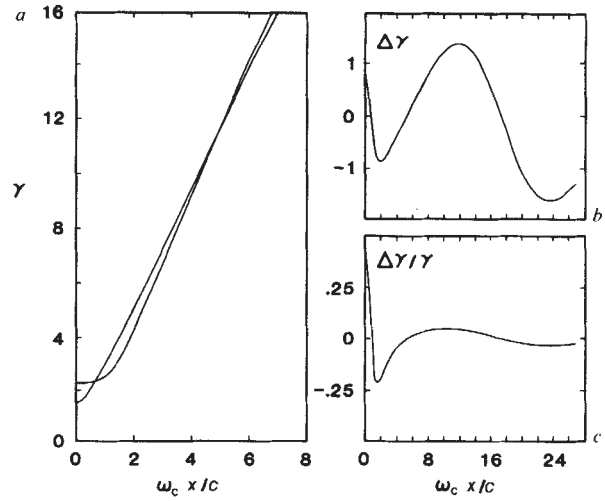

Fig. 5 *a*, Energy gain (γ) plotted against distance for two Surfatron particles of different initial velocities (0.8*c* and 0.9*c*). In *b*, energy separation ($\Delta\gamma$) of the particles remains roughly constant, while in *c*, $\Delta\gamma/\gamma$ decreases rapidly. $V_{ph}/c = .9$, $cE/B = 2.5$, $\omega/\omega_c = 9$. ω_c is the nonrelativistic electron cyclotron frequency.

beam contours at $450/\omega_p$ (Fig. 3*b*). Although the outer contours are still the same size, the contours at the beam centre are seen to 'self-focus' to a smaller size. We have determined that this self-focusing is due to two effects: intensity-dependent refractive index (relativistic self-focusing) and transverse intensity gradient (ponderomotive self-focusing). Whether the beam self-focuses as a whole or breaks up into smaller filaments depends on the transverse size and the intensity profile of the laser beams. In any case, catastrophic self-focusing is an undesirable phenomenon because it tends to push the plasma out and create a channel of low density, thereby destroying the resonance condition for driving the plasma wave and terminating the accelerating process.

Two-dimensional simulations of the beat wave build-up have been encouraging and given results that are consistent with predictions of the fluid and single particle theories. Although there are many competing instabilities in the plasma, these occur on a longer time scale; and plasma wave coherence can be maintained over typically tens of plasma wave wavelengths at the front of the laser pulse, which continually moves into unperturbed plasma. If the laser pulse is longer than this, then wave-particle and wave-wave interactions heat up the plasma to temperatures of hundreds of keV at the back of the laser pulse and make it extremely turbulent. Thus, extremely short laser pulses on the order of a few picoseconds are probably most effective in this acceleration scheme. Such short pulses will also inhibit other instabilities such as the stimulated Brillouin scattering.

Phase-stabilization

The limit on energy gain of a particle in the Plasma beat wave accelerator can be overcome if a magnetic field of appropriate strength, $\gamma_{ph} B < E_{epw}$, is applied perpendicular to the plasma wave (Fig. 4). This accelerates particles parallel to the phase fronts of the accelerating wave, which, in turn, provides a force keeping the particles in phase with the wave[5]. In principle, therefore, particles can gain energy at rate

$$\frac{\Delta U}{\Delta x} = 0.1\left[\frac{B_{KG}}{n_{16}\lambda_\mu}\right](n_{16})^{1/2}\ \text{GeV cm}^{-1} \qquad (4)$$

in the direction of the wave and the accelerated particles move at an angle $\tan\theta = 3\times10^{-3}\sqrt{n_{16}\lambda_\mu}$ with respect to the wavevector of the plasma wave. Here B_{KG} is the applied magnetic field in kilogauss, n_{16} is the plasma density in units of 10^{16} cm^{-3} and λ_μ is the laser wavelength in micrometres. The quantity in the square bracket must be $<\varepsilon$ to prevent the detrapping by the magnetic field. Because the particles move at an angle with respect to the plasma wave, the width of the plasma wave necessary to accelerate the particles to the desired energy can be rather large. Fortunately, the plasma wave width (and hence the energy required to excite it) can be reduced considerably by beating the electromagnetic waves at a finite angle (optical mixing) rather than colinearly[6]. One possible limitation associated with finite angle optical mixing is that, while the particles move at $\sim c$, the laser energy propagates through the plasma with the particles at v_g. In a device of length L the particles move ahead with respect to the laser pulse by a distance $\Delta L = \omega_p^2 L/\omega_0^2$. Thus the plasma wave coherence must be maintained over a distance ΔL behind the leading edge of the laser pulse. We have carried out one-dimensional (one spatial, three velocites) particle simulations, which confirm the above scaling laws. Two-dimensional computer simulations are being carried out to test the phase-locking and cross-field acceleration concept when the plasma wave is driven by finite angle optical mixing, but this technique has the promise of utilizing the high gradients of space-charge plasma waves for obtaining ultrahigh energies. For example, using a 100-kG magnetic field across a 10^{19} cm^{-3} plasma and a 1-μm laser, particles may be accelerated to 100 GeV in a device that is only 3.16 m long.

Laser and plasma requirements

While there is a tremendous promise for >10 MeV cm^{-1} acceleration gradients in this scheme, there are technological obstacles between the concept and a realizable working system. The laser needed for a TeV class accelerator based on this concept will exceed the capability of fusion lasers (presently the largest laser systems) in the areas of peak power, pulse width, repetition rate, and the need for the power to be delivered in a single diffraction limited beam. Considerable work is also needed in the areas of focusing and optical transport of such high peak power leaser beams.

An estimate of the laser power required can be obtained from energy balance arguments. The longitudinal electric field of the plasma wave represents an energy density

$$W_{epw} = \frac{E_{epw}^2}{8\pi} \simeq 500\, n_{16}\varepsilon^2\ \text{J cm}^{-3} \qquad (5)$$

Because the group velocity of the plasma wave, $3v_e^2/v_{ph} \ll c$, we assume that the laser pulse excites the plasma wave only in the

volume through which it propagates. To avoid significant pump depletion, the total energy in the laser beams must be much greater than that in the plasma wave.

The problem of producing plasmas (particularly with a cross magnetic field) with densities between $10^{16} < n_e < 10^{20}$ cm^{-3} and with the required length and homogeneity will also require considerable attention. At high intensities that are necessary in this scheme, the requirement that plasma frequency be exactly equal to the difference frequency may be relaxed, but this issue needs careful investigation.

Prospects for ultrahigh energies

High-phase velocity space charge waves in a plasma have the potential for producing the high accelerating gradients that are necessary for a new generation of particle accelerators. Whether this scheme can be used to accelerate particles to ultrahigh energies depends on how well the phase stabilization (Surfatron) scheme can be made to work in practice. Particular problems are pump depletion, filamentation of the laser and injected particle beams, and the effect of self-generated magnetic fields on the accelerating particles.

On the positive side, the Surfatron scheme would produce a compact accelerator with a high quality beam. The energy spread, $\Delta\gamma/\gamma$ would be small because approximately half of the injected particles quickly form accelerating 'buckets' that are narrow in phase space near the equilibrium point. In the wave frame this is where $\gamma_{ph}B$ is equal to the local longitudinal electric field. Thus all the particles gain energy at nearly the same rate, the one given by equation (4). The bunch length of the final beam as well as $\Delta\gamma/\gamma$ is thus expected to be extremely small, as shown in Fig. 5.

The number of accelerated particles N can be estimated from the consideration of the energy balance[6]:

$$N = 2\times10^{10}\frac{\text{laser energy (kJ)}}{\text{particle energy (GeV)}}\varepsilon\alpha\lambda_\mu\sqrt{n_{16}} \qquad (6)$$

where factor α is the ratio of particle energy to wave energy.

The zero-order motion of the particles in the Surfatron scheme is approximately a straight line, and thus synchrotron radiation loss turns out not be to be a problem. The radiation loss due to high-order bounce motion[5] and due to oscillation in the laser field, as well as other loss mechanisms such as Coulomb scattering and bremsstrahlung radiation, are also not thought to be serious problems.

Finally, the acceleration scheme is still at an embryonic stage for a reliable estimate to be made of its potential total efficiency from wall power (ac) to beam power. The severest limitation, one that is common to all laser acceleration schemes, is the a.c.-to-laser beam efficiency. If we optimistically assume this to be 10% then using our simulations as a guide we may be able to achieve a total efficiency between 10^{-3} and 10^{-4}.

We thank Professor F. F. Chen and Dr C. E. Clayton for valuable comments and discussions. This work was supported at UCLA by DOE contract DE-AM03-76SF00034, NSF grant ECS 83-10972 and LLNL University Research Program and at LANL by the DOE.

Received 11 May; accepted 6 August 1984.

1. Tajima T. & Dawson, J. M. *Phys. Rev. Lett.* **43**, 267–270 (1979).
2. Rosenbluth, M. N. & Liu, C. S. *Phys. Rev. Lett.* **29**, 701–705 (1972).
3. Joshi, C., Tajima, T., & Dawson, J. M., Baldis, H. A. & Ebrahim, N. A. *Phys. Rev. Lett.* **47**, 1285–1288 (1981).
4. Morse, R. L. & Neilson, C. W. *Phys. Fluids* **14**, 830–840 (1971).
5. Katsouleas, T. & Dawson, J. M. *Phys. Rev. Lett.* **51**, 392 (1983).
6. Katsouleas, T., Joshi, C., Mori, W. B. & Dawson, J. M. *Proc. 12th int. Conf. on High-Energy Accelerators* (Fermilab, Batavia, 1982).
7. Cohen, E. I., Kaufman, A. N. & Watson, K. M. *Phys. Rev. Lett.* **29**, 581–584 (1972).

Is there a climatic attractor?

C. Nicolis

Institut d'Aéronomie Spatiale de Belgique, 3 avenue Circulaire, 1180 Bruxelles, Belgium

G. Nicolis

Faculté des Sciences de l'Université Libre de Bruxelles, Campus Plaine, Boulevard du Triomphe, 1050 Bruxelles, Belgium

Much of our information on climatic evolution during the past million years comes from the time series describing the isotope record of deep-sea cores. A major task of climatology is to identify, from this apparently limited amount of information, the essential features of climate viewed as a dynamic system. Using the theory of nonlinear dynamic systems we show how certain key properties of climate can be determined solely from time series data.

EXPERIMENTAL data have essentially two roles in the process of modelling. First, they parameterize the equations postulated by the modeller. Second, they set constraints to be satisfied by the model. For instance, a reasonable model of Quaternary glaciations should reproduce the general aspects of a palaeotemperature time series as deduced from ice or deep-sea core data and, in particular, should exhibit the characteristic time scales of 100,000, 41,000 and 22,000 yr (ref. 1). In either case, however, the information drawn from the data will remain esentially one-dimensional. Thus, starting from the time series of a certain variable one may construct a power spectrum or a histogram which, despite their interest, do not provide any hint about the additional variables that may affect the evolution. We show here that experimental data contain far richer information which, independent of any particular model, can be used to 'resurrect' the multivariable dynamics of a system starting from a time series pertaining to a single variable.

We should first comment on the status of a time series from the standpoint of the theory of dynamical systems. Let $X_0(t)$ be the time series available from the data, and $\{X_k(t)\}$, where $k = 0, 1, \ldots n-1$, the full set of variables actually taking part in the dynamics. $\{X_k\}$ is expected to satisfy a set of first-order nonlinear equations, whose form is generally unknown but which, given a set of initial data $\{X_k(0)\}$, will produce the full details of the system's evolution. It is instructive to visualize this evolution in an abstract multi-dimensional space spanned by these variables, the phase space. An instantaneous state of the system becomes a point, say P, in this space, whereas a sequence of such states followed as time varies defines a curve, the phase space trajectory (see Fig. 1). As time grows and transients die out, the system is expected to reach a state of permanent regime, not necessarily time-independent. In phase space, this will be reflected by the convergence of whole families of phase trajectories towards a subset of phase space (C in Fig. 1), such that the system subsequently remains trapped therein. We refer to this invariant set as the attractor.

The interest of the phase space description of a system lies primarily in the fact that the nature of the attractors provides extensive information on the time behaviour of the variables and on the nature of their coupling. For instance, a point